Vol. 24, No. 2(2025) IA25486
Revista Mexicana de Ingeniería Química

Preparation and characterization of a biocomposite for Cr(VI) adsorption by evaluating the useful life of the biomaterial

Preparación y caracterización de un biocompuesto para la adsorción de Cr(VI) evaluando la vida útil del biomaterial

C. Tejada-Tovar[1]*, Á. Villabona-Ortiz [1], R. Ortega-Toro [2], N. Beleño-Garrido [3], L. Sierra-Payares [3]
[1] Full Professor, Universidad de Cartagena, Faculty of Engineering, Department of Chemical Engineering, Cartagena, Colombia. Process Design, and Biomass Utilization Research Group (IDAB). Avenida del Consulado St. 30. Cartagena de Indias, Colombia, 130015
[2] Full Professor, Universidad de Cartagena, Faculty of Engineering, Department of Food Engineering, Cartagena, Colombia. Food Engineering Department, Food Packaging and Shelf-Life Research Group (FP&SL). Avenida del Consulado St. 30. Cartagena de Indias 130015, Colombia
[3] Chemical Engineering, Universidad de Cartagena, Faculty of Engineering, Department of Chemical Engineering, Cartagena, Colombia. Process Design, and Biomass Utilization Research Group (IDAB). Avenida del Consulado St. 30. Cartagena de Indias, Colombia, 130015
Received: December 14, 2024; Accepted: April 25, 2025

Abstract
The objective of this work was to prepare and characterize a biocomposite made from plantain pseudo stem (PSP), agro-industrial waste and polylactic acid (PLA) for potential use in removing Cr(VI) from solution. Cellulose (CL) was extracted from the plantain pseudo stem waste and modified with PLA. The effect of adsorbent dosage on adsorption efficiency at different concentrations was evaluated, and an adsorption-desorption study was conducted to determine the biocomposite's lifetime. FTIR, SEM and TGA-DSC analyses were performed. The results showed that the plant fiber was successfully modified with PLA, resulting in the formation of the PSP/PLA biocomposite. It was observed that the adsorbent dosage affected the adsorption process, with the best removal efficiencies being 51.74% at 65 mg/L and 49.74% at 30 mg/L at an optimal pH of 2. Adsorption-desorption cycles showed that the biocomposite can be reused up to twice. The inherent properties of the plant fiber were critical, and the crosslinking agent enhanced the biomaterial's performance. This biocomposite shows potential for removing metal contaminants from the solution, thereby contributing to the increased utilization of waste biomass.
Keywords: Polylactic acid, Biocomposite, Cellulose, plantain pseudo stem, Agricultural waste.

Resumen
El objetivo de este trabajo fue la preparación y caracterización de un biocompuesto a partir de residuos agroindustriales de pseudotallo de plátano (PSP) y ácido poliláctico (PLA) con potencial uso en la remoción de Cr (VI) en solución. Se realizó un proceso de extracción y modificación de celulosa con PLA. Se evaluó el efecto de la dosis de adsorbente sobre la eficiencia de adsorción a distintas concentraciones, y se realizó un estudio de adsorción-desorción para determinar la vida útil del biocompuesto. Se realizaron análisis de caracterización FTIR, SEM y TGA-DSC. Los resultados mostraron la exitosa modificación de la fibra vegetal con PLA, dando lugar a la formación del biocompuesto PSP/PLA. Se observó que la dosis de adsorbente afecta el proceso de adsorción, siendo las mejores eficiencias del 51.74% para 65 mg/L y del 49.74% para 30 mg/L a un pH óptimo de 2. Los ciclos de adsorción-desorción determinaron que el biocompuesto posee una reutilización máxima de 2 veces. Las propiedades inherentes de la fibra vegetal fueron fundamentales, y el agente entrecruzante mejoró el desempeño del biomaterial. Este biocompuesto muestra potencial para la eliminación de contaminantes metálicos en solución, contribuyendo a reducir la brecha en el uso de biomasas residuales.
Palabras clave: Ácido poliláctico, Biocompuesto, Celulosa, Pseudotallo de plátano, Residuos agrícolas.

* *Corresponding author. E-mail*: ctejadat@unicartagena.edu.co ;
https://doi.org/10.24275/rmiq/IA25486
ISSN:1665-2738, *issn-e*: 2395-8472

1 Introduction

In recent years, suitable solutions have been sought for the utilization of agro-industrial waste generated by various industries worldwide to reduce their environmental impact. Collectively, the United States, India, and China generate approximately 1,550 million tons of agricultural waste annually, with China being the largest producer (Kumar Sarangi *et al*., 2023; McNeill *et al*., 2024). Much of this waste represents a valuable source of biomass for the production of value-added products, contributing to environmental sustainability and the circular economy by reducing the accumulation of agricultural residues and offering an alternative to fossil-based materials (Kumar Sarangi *et al*., 2023). The waste generated includes sugarcane bagasse, coconut shells, wheat husks, jute fibers, peanut shells, plantain peels, cassava peels, yam peels, and oil palm residues (Nata *et al*., 2024; Saifullah *et al*., 2024; Tejada-Tovar *et al*., 2019). To take advantage of these biomasses, the synthesis of composite materials has been proposed as an alternative that contributes to environmental protection, with potential applications in the development of biodegradable packaging and wastewater treatment due to their biological origin (Saifullah *et al*., 2024; Sherugar *et al*., 2022). For use in treating contaminated water, waste biomasses are transformed into porous surface-active adsorbent biocomposites capable of retaining both organic and inorganic contaminants. However, the use of residual fiber alone is not sufficient to produce highly efficient materials; therefore, natural fibers are combined with a polymeric matrix to enhance their physicochemical properties and increase the adsorption capacity of the materials. This positions them as a promising alternative due to their low cost, environmental friendliness, and high efficiency (Zarna *et al*., 2021; Zheng *et al*., 2024).

Plantain pseudo stem (PSP) is a lignocellulosic natural fiber commonly used in the preparation of biocomposites due to the presence of hydroxyl and carboxyl functional groups that facilitate the removal of contaminants from solutions (Selimin *et al*., 2022). An effective method for preparing PSP-based biocomposites involves crosslinking the vegetable fiber with a modifying agent such as polylactic acid (PLA). PLA provides good thermal and mechanical resistance, which enhances the adhesion characteristics of the biomaterial, modifies its hydrophilic properties to hydrophobic ones, and improves its efficiency in adsorbing pollutants from solutions (Kadea *et al*., 2024; Vatanpour *et al*., 2022).

Chromium is a heavy metal that has been widely studied due to its classification as one of the most toxic pollutants and its high prevalence in various industrial processes. Chromium in its hexavalent form, Cr(VI), is among the most common and hazardous species found in the environment (Diaz-Rodriguez *et al*., 2025). Its level of toxicity poses a serious threat to all living organisms, causing conditions such as stomach ulcers, anemia, and disorders of the lungs, kidneys, liver, and even the reproductive system. In addition to its mutagenic and teratogenic effects, Cr(VI) exhibits high environmental mobility due to its strong oxidizing potential and high solubility (Islam *et al*., 2020; Zhao *et al*., 2023). Exposure to this chemical increases the risk of developing various types of cancer, including stomach, colon, and lung cancer. As a result, environmental protection agencies have established permissible concentration limits for Cr(VI) in water. According to the U.S. EPA, the maximum allowable concentration of chromium is 0.05 mg/L in drinking water and 0.1 mg/L in surface water (Khan *et al*., 2016; Zhao *et al*., 2023).

The literature does not report many applications of converting waste biomass into PLA-modified materials for use in metal removal. For example, Luqman. *et al*., 2020 developed a biocomposite film using cellulose derived from banana fiber, and PLA, and characterized their morphological and crystalline properties by SEM and XRD respectively. Analyzing the results obtained, PLA/plantain cellulose seemed to increase the thermal stability of the biocomposite film. Similarly, Yang *et al*., 2024 developed a biocomposite from a mixture of starch, cellulose, and PLA. The prepared biocomposite showed good hydrophobic properties and excellent mechanical properties, improving the tensile strength from 2.09 MPa to 3.53 MPa. On the other hand, Madenli *et al*., 2023 prepared a biocomposite based on fungal hyphae (*Aspergillus oryzae* and *Penicillium roqueforti*) for the removal of Cr(VI). The results showed a removal efficiency of 98.9% of the contaminant within 11 hours and Moreno-Rubio *et al*., 2025, used Luffa as a bioadsorbent material to remove Cr(VI) from synthetic waters. The prepared material was characterized by SEM and FTIR analysis. The results obtained showed the presence of mainly C and O, while FTIR identified hydroxyl, carbonyl and carboxyl functional groups. It was also obtained that Luffa is composed of 14% lignin, 76% cellulose and 10% hemicellulose. Finally, the adsorption process obtained an efficiency of 100% of Cr(VI) in a period of 1416 hours.

Considering the importance of developing new materials using waste biomass generated by various anthropogenic activities, this research aims to prepare and characterize a biocomposite based on PSP and PLA for the removal of Cr(VI) from solution, positioning it as an adsorbent material that contributes to closing the existing gap in the utilization of agro-industrial waste for potential applications in pollutant adsorption processes.

2 Methodology

2.1 Materials and reagents

Plantain pseudo stem from agro-industrial waste collected in the city of Cartagena, Colombia, and PLA $(C_3H_4O_2)_n$ purchased from Nature Works were used as raw materials in the preparation of the biocomposite. PLA served as the modifying agent. Sodium hydroxide (NaOH), supplied by EMSURE, was used for alkaline extraction; sodium chlorite ($NaClO_2$) and glacial acetic acid (CH_3COOH) were employed for cellulose purification; and sulfuric acid (H_2SO_4), also from EMSURE, was used to obtain cellulose acetate (CA). Additional materials used included hydrochloric acid, acetic anhydride, dichloromethane, acetone, a heating plate with magnetic stirrer, analytical balance, oven, sieve shaker, and electric mill.

2.2 Obtaining cellulose acetate

To obtain cellulose acetate, a pre-treatment of the plantain pseudo stem fiber was first carried out. The fiber was sourced from a plantation in the city of Cartagena. It underwent a process of peeling, washing, and air-drying for three days. After drying, the fiber was milled to reduce its size and then sieved to obtain the desired particle size. Cellulose extraction was performed through a double alkaline treatment using 2 wt.% NaOH for 45 minutes at a temperature of 75 °C to remove lignin, hemicellulose, and other impurities. Considering the solid-to-liquid ratio, 20 g of NaOH and 20 g of pretreated fiber were added to one liter of solution. This process was carried out in duplicate. The fibers were then thoroughly washed with water until a neutral pH of 7 was reached and subsequently dried at 60 °C for 24 hours (Joshi *et al*., 2024; Melikoğlu *et al*., 2019).

Subsequently, 500 mL of distilled water were used to prepare a bleaching solution by adding 50 mL of glacial acetic acid (CH_3COOH) and 50 g of sodium chlorite ($NaClO_2$), with magnetic stirring at 200 rpm for 24 hours to carry out the bleaching of the cellulose. The recovered material was filtered, washed to a neutral pH (7), and dried for 24 hours at 50 °C (González-Delgado *et al*., 2022; Melikoğlu *et al*., 2019).

Finally, to obtain CA, 10 g of CL were mixed with 25 mL of CH_3COOH and stirred at 160 rpm for 30 minutes at 35 °C. To the resulting mixture, 40 mL of CH_3COOH and 0.08 mL of sulfuric acid (H_2SO_4) at 95% concentration were added, followed by an additional 45 minutes of stirring. Then, a solution of 40 mL of acetic anhydride and 0.6 mL of H_2SO_4 was added to the mixture, which was maintained under stirring for 1.5 hours. Afterward, 10 mL of distilled water and 20 mL of CH_3COOH were added, and the mixture was kept under agitation for 20 hours. The final material obtained from this entire process was filtered under vacuum, washed with distilled water, and dried at 35 °C for 48 hours (Ortega & Rodríguez, 2018). This methodology is illustrated in Figure 1.

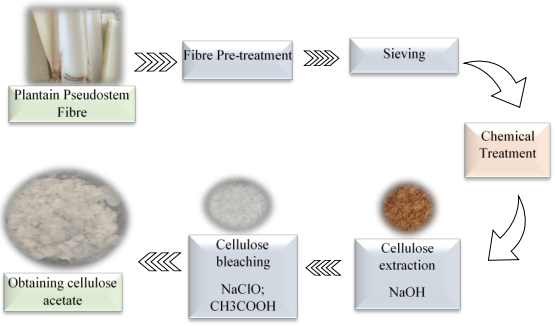

Figure 1. Methodology for obtaining CA.

Once the CA was obtained, it was washed with plenty of distilled water until a neutral pH (7) was obtained and then dried at room temperature for 48 hours.

2.3 Preparation of the biocomposite

Two solutions were prepared: the first containing 50 mL of dichloromethane and 1.8 g of PLA, and the second containing 50 mL of acetone and 5 g of the obtained CA. Each solution was poured into a glass container with a lid and subsequently subjected to ultrasound treatment for 45 minutes at 60 °C. After the designated time, 17 mL of the first solution and 50 mL of the second were taken and evenly combined in a Petri dish. Finally, the mixture was left to stand at room temperature for 24 hours to allow for solvent evaporation (Abu Aldam *et al*., 2020).

2.4 Parametric study

A parametrization study was carried out, evaluating two factors: the initial concentration of the pollutant (C_i) and the amount of adsorbent (X_i). The operating ranges evaluated are shown in Table 1.

Table 1. Study parameters and ranges.

Parameter	Range	Unit
C_i	30 65 100	(mg/L)
X_i	10 20 30	(mg)

2.5 Characterization of the biocomposite

The biocomposite surface charges were studied by means of pHpzc Fourier Transform Infrared Spectroscopy (FTIR) analysis was also carried out to identify the functional groups involved in the materials, using the IRAffinity-1 FTIR Shimadzu equipment, serial number A213749. The morphology and surface composition of the biocomposite were studied by SEM analysis using a TESCAN MIRA3 model. Thermogravimetric analysis and DSC were performed to determine thermal stability, using a TA Instruments thermogravimetric analyzer, serial number 0600-11099, model SDT Q600, with a heating ramp of 10 °C/min, alumina crucibles, and a flow rate of 20 cm^3/min.

2.6 Point of zero charge (pHpzc)

The point of zero charge of the synthesized PSP/PLA biocomposite was determined to establish the pH at which it has the greatest capacity to retain contaminants on the surface. Eighteen test tubes were used, including replicates, each containing 0.01 g of biocomposite, to which 10 mL of $K_2Cr_2O_7$ solution at 100 ppm was added. The pH of each solution in the test tubes was adjusted with 0.1 M HCl and 0.1 M NaOH over a range from pH 2 to pH 10, and the samples were shaken for 24 hours in a shaker (Iheanacho *et al*., 2023). After the set time, the pH of each sample, both original and replicate, was measured.

2.7 Biocomposite reuse study

A study was carried out to evaluate the reusability and regeneration of the synthesized Cr(VI)-loaded biocomposite using an adsorption–desorption cycling process with NaOH and HCl solutions. For this purpose, 30 mL solutions of 0.2 M HCl and NaOH (separately) were prepared, and each of these solutions was placed in contact with 0.5 g of residual biomaterial recovered from the adsorption tests for 2 hours under stirring at 140 rpm. The material was then washed and dried in an oven at 100 °C for 20 minutes. The resulting biomaterial was tested with Cr(VI) solutions at 100 mg/L under agitation at 140 rpm for 2 hours. To measure the reuse efficiency, the absorbance was measured using a UV-Vis spectrophotometer by the diphenyl carbazide method (Badawy *et al*., 2023). This process was performed in triplicate.

3 Results and discussion

3.1 Synthesis of PSP/PLA composite biomaterial

According to the proposed methodology, Figure 2 shows the synthesized PSP/PLA biocomposite. During the synthesis process, the alkaline extraction of CL showed a brown color attributable to lignin and impurities remaining in the plantain stem fiber, which were subsequently removed through the alkaline process. With the bleaching process, the lignin present was eliminated by oxidation, resulting in purified CL. The alkaline extraction technique and the formation of CA were used to successfully modify PSP/PLA from 20 g of plantain pseudo stem fiber, obtaining 18 g of CL in the extraction process and 6 g of PSP/PLA biocomposite.

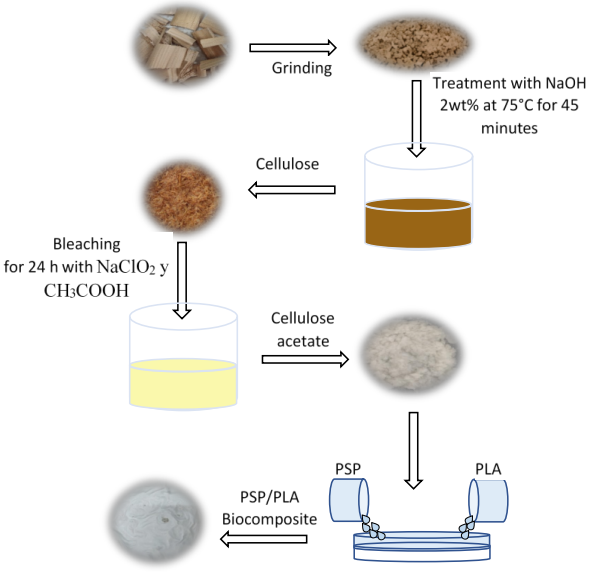

Figure 2. Synthesized PSP/PLA Biocomposite.

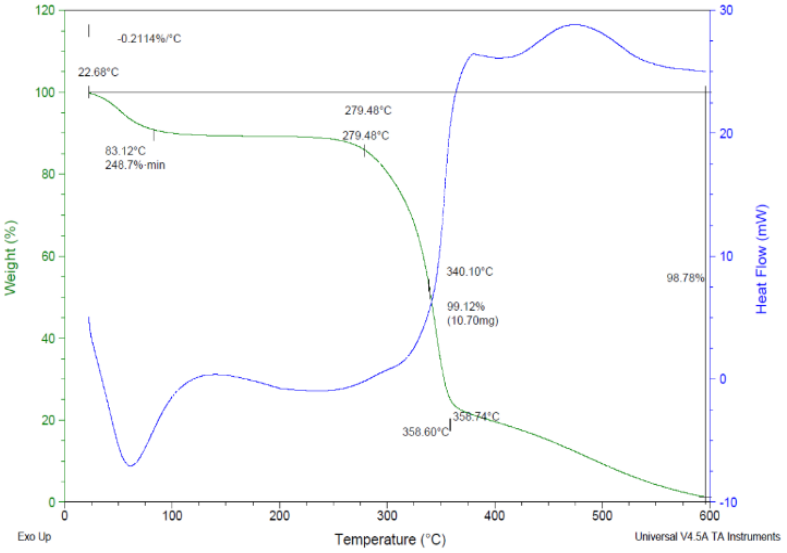

Figure 3. TGA-DSC analysis of CL extracted from plantain pseudo stem

The results showed good yield throughout the fiber utilization process, achieving 90% for the extraction of CL and 100% for the synthesis of the biocomposite. These results are consistent with those reported in previous studies on the CL fraction obtained from the plantain stem, where Thi Thuy Van *et al*., 2022 and Meng *et al*., 2019, obtained efficiencies of 82.136% and 91.33%, respectively. Regarding the mixture of CA with PLA, recent research shows that a higher content of CL improves the mechanical properties of the material, such as tensile strength and elasticity. Additionally, it improves its hydrophobic properties and its amorphous nature, as specified in the study conducted by Abu Aldam *et al*., 2020.

3.2 *Thermogravimetric analysis - TGA*

In order to analyze the purity, thermal, and stability properties of the CL extracted from plantain stem fiber, a TGA-DSC analysis was carried out over a temperature range from 0 °C to 600 °C with a heating ramp of 10 °C/min and a flow rate of 20 cm^3/min. The results obtained from the analysis are shown in Figure 3, where it is observed that the thermal stability of the plantain stem CL is reached at 22 °C, with a slight mass loss between 23–83 °C, which can be attributed to the evaporation of contained water and adsorbed moisture from the environment (Mi & Wang, 2024). The onset of decomposition occurs between 279.48 °C and 358.74 °C, with a significant mass loss, reaching 99.12% at 340.10 °C, which can be attributed to the degradation of lignin, CL, and hemicellulose still present in the sample (Satha *et al*., 2020). These results are consistent with those reported by Gupta & Raghav, 2020, who observed similar behavior in terms of weight loss and degradation of CL obtained from *Citrus limetta*, recording a degradation temperature between 165 °C and 390 °C. Similarly, Shrestha *et al*., 2021, obtained comparable results for weight loss and degradation of CL extracted from plantain stem, reporting a degradation temperature range of 228 °C to 384 °C.

3.3 *Point of charge pHpzc*

Figure 4 presents the results obtained in the determination of pHpzc for the synthesized PSP/PLA biocomposite. The determination of the point of zero charge is of great importance, as it helps to understand the electrical charges of the biomaterial, which are dependent on the pH of the solution and related to the ionization of functional groups on the surface of the adsorbent (Aigbe & Osibote, 2021; Rodríguez *et al*., 2010). The results showed that for PSP/PLA, the pHpzc exhibited a value of 8, indicating that at this value the surface charge of the adsorbent is zero (Tejada-Tovar *et al*., 2023). It is important to mention that electrostatic interaction favors the adsorption of anionic species when the pH of a solution is lower than the point of zero charge (pHpzc), while covalent interactions facilitate the adsorption of cationic compounds when the pH of the solution is higher than the pHpzc (Labied *et al*., 2018). Studies reported in the literature have highlighted the importance of pH in the adsorption of heavy metals. For example, Yadav *et al*., 2024, showed that the optimum pH for the removal of Ni(II) ions is 8. Similarly, in the study by Nurdin *et al*., 2015, cited in Aigbe & Osibote, 2021, they found that the optimum removal of Cd(II), Ni(II), and Cu(II) ions occurs at pH 8. Considering that in aqueous solutions, chromium is generally present as $Cr_2O_7^{2-}$ and $HCrO^{4-}$, carrying out the adsorption at low pH will favor the PSP/PLA biocomposite to have a positively charged surface,

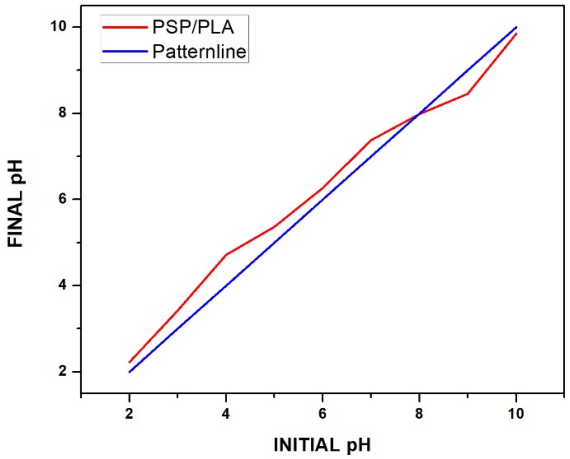

Figure 4. Data obtained from pHpzc.

which will facilitate the adsorption of chromium (Tejada-Tovar *et al*., 2023). Due to this, a pH of 2 was chosen, considering that most related studies are conducted at pH 2–3. For instance, Liang *et al*., 2023, successfully removed Cr(VI) ions using sodium alginate/phosphorus tetramethyl sulfate beads at an optimum pH of 3.

3.4 Fourier Transform Infrared Analysis – FTIR

Fourier Transform Infrared Spectroscopy (FTIR) is a technique used to characterize different types of samples, whether in solutions, pastes, films, powders, fibers, liquids, or gases. Figure 5 shows the FTIR spectra of the plantain pseudo stem vegetable fiber and the synthesized PSP/PLA biocomposite, both before and after the Cr(VI) adsorption test. It is observed that the plantain pseudo stem fiber (Figure 5a) shows peaks between 3300–3500 cm^{-1}, indicating the presence of amines (N–H), and between 3500–3750 cm^{-1}, indicating O–H, which could be due to residual water present in the sample. On the other hand, peaks with strong intensity appear, indicating the presence of a carbonyl group (C=O) between 1690–1760 cm^{-1}, and alkenes (C–H) at lower frequencies (Rahim & Mas Haris, 2022).

On the other hand, the synthesized biocomposite with PLA, presented in Figure 5b, displays more frequent and characteristic peaks. The presence of amines (N-H) is maintained, and a strong absorption band appears between 2850-2970 cm^{-1}, indicating the presence of alkanes (C-H), which consecutively generate other bands that extend down to 1470 cm^{-1}, indicating the stability of the formed molecule. Likewise, aromatic rings (C-H) are observed at lower frequencies, 690-900 cm^{-1}, indicating greater stability and confirming that a homogeneous mixture of the PSP and PLA materials was obtained (Luqman *et al*., 2020; Villabona-Ortíz *et al*., 2024).

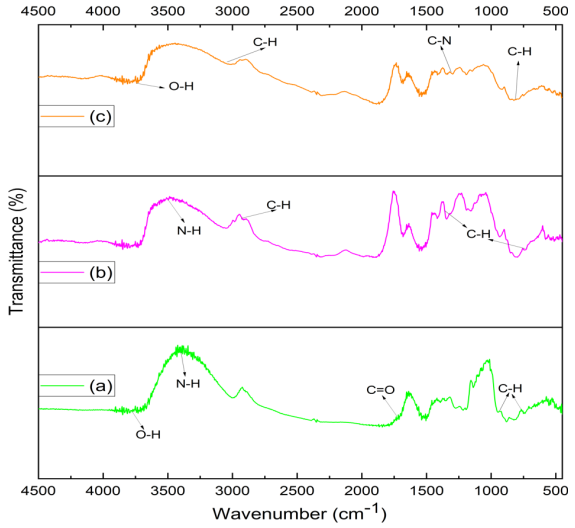

Figure 5. IR Spectra of (a) Plantain pseudo stem fiber, (b) PSP/PLA before adsorption, (c) PSP/PLA after adsorption.

Analysis of the biocomposite after adsorption (Figure 5c) reveals a clear decrease in the characteristic peaks of the functional groups; however, stretching vibrations are still present: a stretching vibration belonging to hydroxyl groups (O-H) is observed between the wavelengths of 3800-3900 cm^{-1}, and peaks characteristic of C-H groups (alkanes) appear between 2890-2940 cm^{-1}. Peaks indicating the presence of amines (C-N) are also evident between 1250-1500 cm^{-1}, which help maintain pH balance by counteracting the acidity of the adsorbed Cr(VI) solutions. Additionally, the presence of aromatic rings (C-H) is observed between 750-1000 cm^{-1}, confirming the stability of the synthesized biocomposite (Hsini *et al*., 2020; Nandiyanto *et al*., 2019). The notable decrease in the intensity of the bands is due to the fact that the pollutant is captured by the active sites of the biocomposite, generating interactions with the functional groups of the adsorbent that cause these changes, which confirms the functionality of the material in the adsorption process (Villabona-Ortíz *et al*., 2024).

3.5 Scanning Electron Microscopy – SEM Analysis

SEM analysis was carried out on the biocomposite prepared before and after the Cr(VI) adsorption test to study its morphological characteristics and understand the effect of the PLA matrix on its behavior. Figure 6 shows the SEM micrographs of the biocomposite before (Figure 6a) and after the adsorption test (Figure 6b). Figure 6a shows the general structure of the biocomposite with more visible fibers, along with a clear distribution and organization of the PSP materials within the PLA matrix. The homogenization

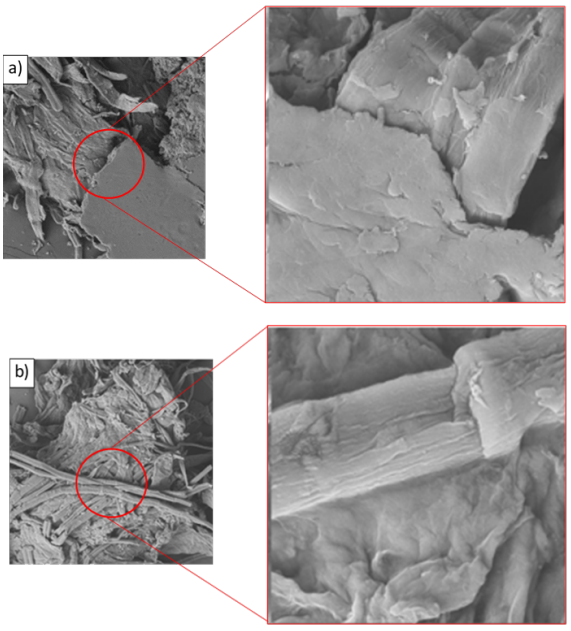

Figure 6. SEM micrographs of PSP/PLA at magnifications of ×500 and ×10,000: (a) before adsorption, (b) after Cr(VI) adsorption.

of the mixture and adhesion between the components can also be observed, resulting in a composite with a rough and fibrous surface in parts, which may confer hydrophobic characteristics and greater tensile strength (Wang *et al*., 2020). These results are similar to those presented by Wan Ishak *et al*., 2020, who synthesized a cellulose–PLA-based biocomposite, and SEM analysis showed a homogeneous mixture of the components with a rough surface. Similarly, Singh *et al*., 2020, developed a biocomposite based on cellulosic fibers and PLA, obtaining similar results in the homogenization of the material mixture and surface roughness of the biocomposite.

After the Cr(VI) adsorption test (Figure 6b), it is observed that the biocomposite presents a more compact surface, with fewer visible pores and brighter areas, suggesting the adhesion of the contaminant to the biocomposite surface, highlighting its capacity for Cr(VI) removal from solution (Fijoł *et al*., 2021).

3.6 Effect of adsorbent dosage on adsorption

The adsorption processes are affected by different parameters, such as temperature, contact time, pH, initial concentration, and stirring speed (Ishtiaq *et al*., 2020). In this study, the adsorption capacity of the synthesized biocomposite was evaluated by varying the adsorbent dose and the initial concentration of the pollutant at pH 2. The adsorbent doses used were 30 mg, 20 mg, and 10 mg. Figure 7 shows the results obtained for the efficiency of the adsorption process (%) as a function of the amount of adsorbent used for the removal of Cr(VI) at initial concentrations

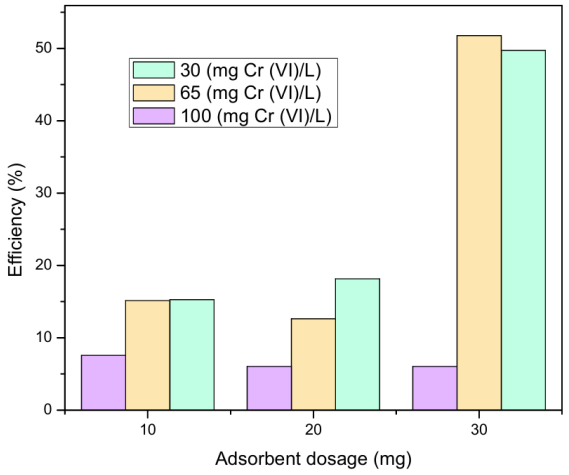

Figure 7. Variation of adsorbent dose at different initial concentrations. a) 30 mg/L, b) 65 mg/L, c) 100 mg/L.

of 30 mg/L, 65 mg/L, and 100 mg/L. It can be observed that, for an initial concentration of 30 mg/L, an efficiency of 49.74% was obtained with a dose of 30 mg of adsorbent, 18.15% with a dose of 20 mg, and 15.29% with a dose of 10 mg. For an initial concentration of 65 mg/L, an efficiency of 51.77% was obtained with a dose of 30 mg of adsorbent, 12.62% with 20 mg, and 15.15% with 10 mg. Finally, for an initial concentration of the pollutant (Cr(VI)) of 100 mg/L, an efficiency of about 6% was obtained with a dose of 30 mg and 20 mg, and an efficiency of 7.57% with a dose of 10 mg. The results showed a trend in which increasing the dose of the synthesized biocomposite led to greater adsorption efficiency, with the best adsorption yield obtained at a contaminant concentration of 65 mg/L and an adsorbent dose of 30 mg. This is due to the fact that a greater presence of adsorbent enhances the removal of a greater amount of contaminant (Shekhawat *et al*., 2023).

3.7 Biomaterial reuse tests

The recovery and reuse of the synthesized biocomposite were evaluated using two Cr(VI) elution agents (0.2 M HCl and 0.2 M NaOH). As shown in Figure 8, the capacity of the biocomposite for efficient Cr(VI) removal was assessed over three adsorption–desorption cycles. It was observed that HCl has the advantage of recovering the surface of the adsorbent more effectively than NaOH. This is due to the fact that HCl reduces the electrostatic interactions generated between the adsorbent and Cr(VI), allowing the release of the metal ions and the recovery of the adsorbent surface for reuse. It is also evident that, with each cycle, the biocomposite significantly reduces its adsorption capacity, especially when using NaOH (Prasad *et al*., 2022).

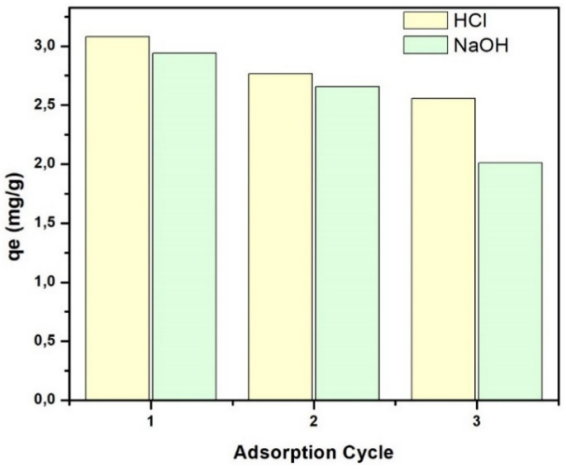

Figure 8. Metal removal in three adsorption cycles.

The results obtained throughout the study suggest that the biocomposite synthesized and modified with PLA represents a promising alternative for the treatment of contaminated water due to its characteristics, including excellent homogeneity in the material mixture, water resistance, thermal stability, good adhesion of the polymeric matrix to the fiber, as well as excellent yield in the synthesis process. In order to provide a broader and more versatile perspective on the PSP/PLA biocomposite, a comparative table (Table 2) is presented, including other studies reported in the literature on the synthesis and characterization of materials derived from agricultural waste. The data presented show consistency between the synthesis and characterization results obtained in this study and those reported by other researchers.

Table 2. Comparison with other studies.

Biomass	Modifying agent	Contaminant removed	Characterization	Reference
Bamboo	Glycidyl methacrylate (GMA)	Cr (VI)	**SEM:** Showed a rough surface on the synthesized material. **FTIR:** 1697–1706 cm^{-1} (C=O stretching vibration), a peak at 1173 cm^{-1} attributed to C–O group stretching, and 814 cm^{-1} (epoxy ring group); peaks between 2929 and 3380 cm^{-1} are due to aliphatic C–H, N–H, and O–H stretching vibrations. The peaks at 2900–3000 cm^{-1} were weakened, which was attributed to the impact of amine, hydroxyl, and aliphatic C–H groups on adsorption. **pH: 2**	(Zhang *et al*., 2022)
Coconut shell	PHB	Methylene blue	**SEM:** The biocomposite presented effective homogenization; it was observed that the biopolymer layers are thin due to increased water resistance in the presence of PHB. **FTIR:** It showed peaks between 3200–3500 cm^{-1}, attributed to single bonds indicating the presence of hydrogen bonds and the vibration of O–H, COOH, and NHx functional groups. Peaks at 2860 cm^{-1} and 2935 cm^{-1} are attributed to aliphatic compounds; peaks between 1650 cm^{-1} and 1850 cm^{-1} suggest the presence of carbonyl groups and aromatic rings; 1490 cm^{-1} and 829 cm^{-1} correspond to C–H, O–H, and C–O bonds. **TGA:** The highest mass loss of coconut cellulose occurs between 250 °C and 350 °C, with a loss of 49.4%, corresponding to the degradation of hemicellulose, lignin, extractives, and lignocellulosic derivatives. **pH:** 8	(Villabona-Ortíz *et al*., 2024)
Passion fruit peels Orange peels Plantain peels	NaOH y $Ca(CH_3CO)_2$	Zinc (II)	**TGA:** 390 °C to 400 °C represents the degradation of cellulose. **FTIR:** Peaks between 3600–3000 cm^{-1} correspond to the hydroxyl group (O–H); 3000–2800 cm^{-1} belong to the stretching of C–H groups; 1744 cm^{-1} and 1638 cm^{-1} correspond to the stretching of COO^- and C=O; peaks between 1430–1455 cm^{-1} indicate C–H groups, and peaks between 1422–1420 cm^{-1} indicate the presence of N–H. **SEM:** It showed a porous structure due to the removal of soluble substances during treatment with alkaline solutions.	(Castro *et al*., 2021)
Potato pulp (PP)	PHBV	-	**SEM:** This indicates that the interfacial adhesion between the PHBV matrix and the PP powder is relatively poor. **TGA:** Thermal degradation occurs in the temperature range of 200 °C to 600 °C and is due to the degradation of hemicellulose, cellulose, and lignin.	(Righetti *et al*., 2019)
Plantain pseudo stem	PLA	-	**FTIR:** A peak between 3300–3500 cm^{-1} indicates the presence of amines (N–H); 2850–2970 cm^{-1} corresponds to C–H stretching; and peaks between 690–900 cm^{-1} indicate greater stability. **SEM:** Homogenization of the mixture and adhesion between the components, resulting in a composite with a rough and partially fibrous surface. **TGA:** The onset of decomposition occurs between 279.48 °C and 358.74 °C, with greater mass loss due to the degradation of lignin, cellulose, and hemicellulose present in the sample. **pH:** 2	Present study

Conclusions

The process of preparation and modification of the PSP/PLA biocomposite was successful, showing that the PLA biopolymer confers hydrophobic properties to the cellulose acetate extracted from the plantain stem, demonstrating that it is possible to cross-link vegetable fibers with biopolymers to produce biocomposites with potential use in the removal of pollutants.

Similarly, the TGA-DSC analysis of the cellulose showed that its decomposition occurs between 279.48 °C and 358.74 °C, with a mass loss of 99%, primarily due to the evaporation of water and moisture content and the degradation of lignin, cellulose, and hemicellulose present in the sample. Additionally, the point of zero charge (pHpzc) for the biocomposite was determined to be 8, indicating that at this pH value, the surface charge of the adsorbent is neutral, which may favor the adsorption of metals when treating solutions with a higher pH.

The results obtained in the adsorption test showed that at a concentration of 65 mg/L and a dose of 30 mg of adsorbent, an efficiency of 51.77% and an adsorption capacity of 3.72 mg/g were achieved. Finally, the characterization of the material revealed that the biocomposite possesses high stability. SEM analysis showed that the biocomposite has a fibrous and compact surface, confirming the presence of the biomass used. Additionally, it was observed that after the adsorption process, Cr(VI) adhered to the surface of the biocomposite, confirming its capacity to remove this contaminant. FTIR analysis also revealed the presence of O–H, C–H, amine (C–N) groups, and aromatic rings (C–N).

Acknowledgements

The authors would like to thank the University of Cartagena for supporting the development of this work.

References

Abu Aldam, S., Dey, M., Javaid, S., Ji, Y., & Gupta, S. (2020). On the synthesis and characterization of polylactic acid, polyhydroxyalkanoate, cellulose acetate, and their engineered blends by solvent casting. *Journal of Materials Engineering and Performance*, *29*(9), 5542–5556. https://doi.org/10.1007/s11665-020-04594-3

Aigbe, U. O., & Osibote, O. A. (2021). Carbon derived nanomaterials for the sorption of heavy metals from aqueous solution: A review. *Environmental Nanotechnology, Monitoring & Management*, *16*, 100578. https://doi.org/10.1016/j.enmm.2021.100578

Badawy, A. M., Farghali, A. A., Bonilla-Petriciolet, A., Selim, A. Q., & Seliem, M. K. (2023). Effective removal of Cr(VI) and methyl orange by nano magnetite loaded starch/muscovite biocomposite: Characterization, experiments, advanced modeling, and physicochemical parameters interpretation. *International Journal of Biological Macromolecules*, *224*, 1052–1064. https://doi.org/10.1016/j.ijbiomac.2022.10.190

Castro, D., Rosas-Laverde, N., Belén Aldás, M., Almeida-Naranjo, C., Guerrero, V. H., & Pruna, A. (2021). Chemical modification of agro-industrial waste-based bioadsorbents for enhanced removal of Zn (II) ions from aqueous solutions. *Materials*, *14*(9), 2134. https://doi.org/10.3390/ma14092134

Diaz-Rodriguez, K. F., Salazar-Pinto, B. M., Flores-Calla, S. S., & Gonzales-Condori, E. G. (2025). Potential use of artichoke (*Cynara cardunculus* L.) waste packed in filter bags for the removal of hexavalent chromium from water. *Revista Mexicana de Ingeniería Química*, *24*(1), 1–21. https://doi.org/10.24275/RMIQ/ia25426

Fijoł, N., Abdelhamid, H. N., Pillai, B., Hall, S. A., Thomas, N., & Mathew, A. P. (2021). 3D-printed monolithic biofilters based on a polylactic acid (PLA) – hydroxyapatite (HAp) composite for heavy metal removal from an aqueous medium. *RSC Advances*, *11*(51), 32408–32418. https://doi.org/10.1039/d1ra05202k

González-Delgado, A., Villabona-Ortíz, A., & Tejada-Tovar, C. (2022). Evaluation of three biomaterials from coconut mesocarp for use in water treatments polluted with an anionic dye. *Water*, *14*(3), 408. https://doi.org/10.3390/w14030408

Gupta, R. D., & Raghav, N. (2020). Nano-crystalline cellulose: Preparation, modification and usage as sustained release drug delivery excipient for some non-steroidal anti-inflammatory drugs. *International Journal of Biological Macromolecules*, *147*, 921–930. https://doi.org/10.1016/j.ijbiomac.2019.10.057

Hsini, A., Essekri, A., Aarab, N., Laabd, M., Ait Addi, A., Lakhmiri, R., & Albourine, A. (2020).

Elaboration of novel polyaniline@Almond shell biocomposite for effective removal of hexavalent chromium ions and Orange G dye from aqueous solutions. *Environmental Science and Pollution Research*, *27*(13), 15245–15258. https://doi.org/10.1007/s11356-020-08039-1

Iheanacho, O. C., Nwabanne, J. T., Obi, C. C., Igwegbe, C. A., Onu, C. E., & Dahlan, I. (2023). Adsorptive dephenolization of aqueous solutions using thermally modified corn cob: mechanisms, point of zero charge, and isosteric heat studies. *Adsorption Science and Technology*, *2023*. https://doi.org/10.1155/2023/2813663

Ishtiaq, F., Bhatti, H. N., Khan, A., Iqbal, M., & Kausar, A. (2020). Polypyrole, polyaniline and sodium alginate biocomposites and adsorption-desorption efficiency for imidacloprid insecticide. *International Journal of Biological Macromolecules*, *147*, 217–232. https://doi.org/10.1016/j.ijbiomac.2020.01.022

Islam, M. A., Angove, M. J., Morton, D. W., Pramanik, B. K., & Awual, M. R. (2020). A mechanistic approach of chromium (VI) adsorption onto manganese oxides and boehmite. *Journal of Environmental Chemical Engineering*, *8*(2), 103515. https://doi.org/10.1016/j.jece.2019.103515

Joshi, M., Dwivedi, C., & Manjare, S. (2024). A renewable cellulose-rich biofiller material extracted from waste banana stem fibers for reinforcing natural rubber composites. *Journal of Materials Science*, *59*(2), 519–534. https://doi.org/10.1007/s10853-023-09230-8

Kadea, S., Kittikorn, T., & Hedthong, R. (2024). Sustainable laminate biocomposite of wood pulp/PLA with modified PVA-MFC compatibilizer: Weathering resistance and biodegradation in soil. *Industrial Crops and Products*, *218*, 118913. https://doi.org/10.1016/j.indcrop.2024.118913

Khan, T., Isa, M. H., Mustafa, M. R., Yeek-Chia, H., Baloo, L., Abd Manan, T. S. B., & Saeed, M. O. (2016). Cr(VI) adsorption from aqueous solution by an agricultural waste based carbon. *RSC Advances*, *6*(61), 56365–56374. https://doi.org/10.1039/c6ra05618k

Kumar Sarangi, P., Subudhi, S., Bhatia, L., Saha, K., Mudgil, D., Prasad Shadangi, K., Srivastava, R. K., Pattnaik, B., & Arya, R. K. (2023). Utilization of agricultural waste biomass and recycling toward circular bioeconomy. *Environmental Science and Pollution Research*, *30*(4), 8526–8539. https://doi.org/10.1007/s11356-022-20669-1

Labied, R., Benturki, O., Eddine Hamitouche, A. Y., & Donnot, A. (2018). Adsorption of hexavalent chromium by activated carbon obtained from a waste lignocellulosic material (*Ziziphus jujuba* cores): Kinetic, equilibrium, and thermodynamic study. *Adsorption Science & Technology*, *36*(4), 1066–1099. https://doi.org/10.1177/0263617417750739

Liang, S., Cai, W., Dang, C., Peng, X., Luo, Z., & Wei, X. (2023). Synthesis of sodium alginate/phosphorus tetramethylmethyl sulfate biocomposite beads with exceptional adsorption rate for Cr(VI) removal. *Journal of Environmental Chemical Engineering*, *11*(2), 109317. https://doi.org/10.1016/j.jece.2023.109317

Luqman., M., Vesuanathan, T. A., & Salleh, M. N. (2020). Isolation and characterization of microcrystalline cellulose extracted from banana fiber in poly(lactic acid) biocomposite produced from solvent casting technique. *IOP Conference Series: Materials Science and Engineering*, *957*(1), 012005. https://doi.org/10.1088/1757-899x/957/1/012005

Madenli, Ö., Akarsu, C., & Deveci, E. Ü. (2023). Effective removal of hexavalent chromium by novel modified alginate-based biocomposites: Characterization, kinetics and equilibrium studies. *Ceramics International*, *49*(10), 16440–16450. https://doi.org/10.1016/j.ceramint.2023.02.005

McNeill, D. C., Pal, A. K., Nath, D., Rodriguez-Uribe, A., Mohanty, A. K., Pilla, S., Gregori, S., Dick, P., & Misra, M. (2024). Upcycling of ligno-cellulosic nutshells waste biomass in biodegradable plastic-based biocomposites uses-a comprehensive review. *Composites Part C: Open Access*, 100478. https://doi.org/10.1016/j.jcomc.2024.100478

Melikoğlu, A. Y., Bilek, S. E., & Cesur, S. (2019). Optimum alkaline treatment parameters for the extraction of cellulose and production of cellulose nanocrystals from apple pomace. *Carbohydrate Polymers*, *215*, 330–337. https://doi.org/10.1016/j.carbpol.2019.03.103

Meng, F., Wang, G., Du, X., Wang, Z., Xu, S., & Zhang, Y. (2019). Extraction and characterization of cellulose nanofibers and

nanocrystals from liquefied banana pseudo-stem residue. *Composites Part B: Engineering*, *160*, 341–347. https://doi.org/10.1016/j.compositesb.2018.08.048

Mi, B., & Wang, Y. (2024). Performance and mechanism of porous carbons derived from biomass as adsorbent for removal of Cr(VI). *Processes*, *12*(10), 2229. https://doi.org/10.3390/pr12102229

Moreno-Rubio, J. G., Osornio-Rubio, N. R., Jiménez-Islas, H., Barrera-Calva, E., Ramírez-Yañez, A. Y., & Martínez-González, G. M. (2025). Characterization and efficiency of Luffa cylindrica as bioadsorbent in Cr (VI) remotion from synthetic wastewater. *Revista Mexicana de Ingeniera Quimica*, *24*(2), 1–14. https://doi.org/10.24275/rmiq/Mat25443

Nandiyanto, A., Oktiani, R., & Ragadhita, R. (2019). How to read and interpret FTIR spectroscope of organic material. *Indonesian Journal of Science and Technology*, *4*(1), 97–118. https://doi.org/10.17509/ijost.v4i1.15806

Nata, I., Irawan, C., Hudha, M. I., Lesti, A., Syarkani, M. H., & Naufal, A. (2024). Enhanced copper ion adsorption by rice husk and sugarcane bagasse-based magnetic nanoparticles biocomposites. *ASEAN Journal of Chemical Engineering*, *24*(1), 79–89. https://doi.org/10.22146/ajche.12236

Nurdin, S., Roslan, A., Abbakar, M. S. A., Khairuddin, S. A., & Sukri, H. A. M. (2015). Rock melon activated carbon (RMAC) for removal of Cd(II), Ni(II) and Cu(II) from wastewater: kinetics and adsorption equilibrium. *International Journal of Chemical Engineering and Applications*, *6*(2), 105–110. https://doi.org/10.7763/ijcea.2015.v6.461

Ortega, G. S., & Rodríguez, A. E. (2018). Síntesis de acetato de celulosa y rayón a partir de residuos agroindustriales del cultivo y procesamiento de piña. *Revista Teinnova*, *3*, 22–28.

Prasad, P. S., Gomathi, T., Sudha, P. N., Deepa, M., Rambabu, K., & Banat, F. (2022). Biosilica/Silk Fibroin/Polyurethane biocomposite for toxic heavy metals removal from aqueous streams. *Environmental Technology and Innovation*, *28*, 102741. https://doi.org/10.1016/j.eti.2022.102741

Rahim, M., & Mas Haris, M. R. H. (2022). Banana trunk fibers-infused acidified chitosan-based biocomposite for Cadmium(II) sorption. *Journal of Natural Fibers*, *19*(13), 4908–4922. https://doi.org/10.1080/15440478.2020.1870636

Righetti, M. C., Cinelli, P., Mallegni, N., Stäbler, A., & Lazzeri, A. (2019). Thermal and mechanical properties of biocomposites made of poly(3-hydroxybutyrate-co-3-hydroxyvalerate) and potato pulp powder. *Polymers*, *11*(2), 308. https://doi.org/10.3390/polym11020308

Rodríguez, A., Ovejero, G., Sotelo, J. L., Mestanza, M., & García, J. (2010). Adsorption of dyes on carbon nanomaterials from aqueous solutions. *Journal of Environmental Science and Health, Part A* , *45*(12), 1642–1653. https://doi.org/10.1080/10934529.2010.506137

Saifullah, A., Chacko, N. G., Dhakal, H. N., Khan, S. H., Sarker, F., & Zhang, Z. (2024). Valorisation of agricultural residue bio-mass date palm fibre in dry-blended polycaprolactone (PCL) bio-composites for sustainable packaging applications. *Waste and Biomass Valorization*, 1–13. https://doi.org/10.1007/S12649-024-02550-z

Satha, H., Kouadri, I., & Benachour, D. (2020). Thermal, structural and morphological studies of cellulose and cellulose nanofibers extracted from bitter watermelon of the cucurbitaceae family. *Journal of Polymers and the Environment*, *28*(7), 1914–1920. https://doi.org/10.1007/S10924-020-01735-6

Selimin, M. A., Latif, A. F. A., Er, Y. C., Muhamad, M. S., Basri, H., & Lee, T. C. (2022). Adsorption efficiency of banana blossom peels (*musa acuminata colla*) adsorbent for chromium (VI) removal. *Materials Today: Proceedings*, *57*, 1262–1268. https://doi.org/10.1016/j.matpr.2021.10.502

Shekhawat, A., Jugade, R., Gomase, V., Kahu, S., Dhandayutham, S., & Pandey, S. (2023). Adsorptive removal of As (III) by cellulose-Sn (IV) biocomposite. *Journal of Composites Science*, *7*(1), 19. https://doi.org/10.3390/jcs7010019

Sherugar, P., Padaki, M., Naik, N. S., George, S. D., & Murthy, D. H. (2022). Biomass-derived versatile activated carbon removes both heavy metals and dye molecules from wastewater with near-unity efficiency: Mechanism and kinetics. *Chemosphere*, *287*, 132085. https://doi.org/10.1016/j.chemosphere.2021.132085

Shrestha, P., Sadiq, M. B., & Anal, A. K. (2021). Development of antibacterial biocomposites reinforced with cellulose nanocrystals derived from banana pseudostem. *Carbohydrate Polymer Technologies and Applications*, *2*, 100112. https://doi.org/10.1016/j.carpta.2021.100112

Singh, A. A., Genovese, M. E., Mancini, G., Marini, L., & Athanassiou, A. (2020). Green processing route for polylactic acid–cellulose fiber biocomposites. *ACS Sustainable Chemistry and Engineering*, *8*(10), 4128–4136. https://doi.org/10.1021/acssuschemeng.9b06760

Tejada-Tovar, C., Gonzalez-Delgado, A. D., & Villabona-Ortiz, A. (2019). Characterization of residual biomasses and its application for the removal of lead ions from aqueous solution. *Applied Sciences*, *9*(21), 4486. https://doi.org/10.3390/app9214486

Tejada-Tovar, C., Villabona-Ortíz, Á., & Ortega-Toro, R. (2023). Removal of metals and dyes in water using low-cost agro-industrial waste materials. *Applied Sciences*, *13*(14), 8481. https://doi.org/10.3390/app13148481

Van, T. T., Gaspillo, P., Thanh, H. G. T., Nhi, N. H. T., Long, H. N., Tri, N., Van, T. T. N., Nguyen, T. T., & Huynh, K. P. H. (2022). Cellulose from the banana stem: optimization of extraction by response surface methodology (RSM) and charaterization. *Heliyon*, *8*(12), e11845. https://doi.org/10.1016/j.heliyon.2022.e11845

Vatanpour, V., Dehqan, A., Paziresh, S., Zinadini, S., Zinatizadeh, A. A., & Koyuncu, I. (2022). Polylactic acid in the fabrication of separation membranes: A review. *Separation and Purification Technology*, *296*, 121433. https://doi.org/10.1016/j.seppur.2022.121433

Villabona-Ortíz, Á., Ortega-Toro, R., & Pedroza-Hernández, J. (2024). Biocomposite based on polyhydroxybutyrate and cellulose acetate for the adsorption of methylene blue. *Journal of Composites Science*, *8*(7), 234. https://doi.org/10.3390/jcs8070234

Wan-Ishak, W. H., Rosli, N. A., & Ahmad, I. (2020). Influence of amorphous cellulose on mechanical, thermal, and hydrolytic degradation of poly(lactic acid) biocomposites. *Scientific Reports*, *10*(1), 1–13. https://doi.org/10.1038/s41598-020-68274-x

Wang, Q., Ji, C., Sun, J., Zhu, Q., & Liu, J. (2020). Structure and properties of polylactic acid biocomposite films reinforced with cellulose nanofibrils. *Molecules*, *25*(14), 3306. https://doi.org/10.3390/molecules25143306

Yadav, N., Saini, O., Debnath, N., Singh, S., Thakur, T. K., Rajendra, K., Meena, R., Thakur, I. S., & Srivastava, S. (2024). Optimizing enhanced heavy metal detoxification by novel hybrid fungal hyphae-nano-biocomposite functionalized with graphene oxide: Unravelling process parameters & adsorption modelling. *Process Safety and Environmental Protection*, *188*, 917–928. https://doi.org/10.1016/j.psep.2024.05.086

Yang, J., Li, Y., Li, X., Ji, M., Peng, S., Man, J., Zhou, L., Li, F., & Zhang, C. (2024). Starch-fiber foaming biodegradable composites with polylactic acid hydrophobic surface. *International Journal of Biological Macromolecules*, *267*, 131406. https://doi.org/10.1016/j.ijbiomac.2024.131406

Zarna, C., Opedal, M. T., Echtermeyer, A. T., & Chinga-Carrasco, G. (2021). Reinforcement ability of lignocellulosic components in biocomposites and their 3D printed applications–a review. *Composites Part C: Open Access*, *6*, 100171. https://doi.org/10.1016/j.jcomc.2021.100171

Zhang, Y. N., Guo, J. Z., Wu, C., Huan, W. W., Chen, L., & Li, B. (2022). Enhanced removal of Cr(VI) by cation functionalized bamboo hydrochar. *Bioresource Technology*, *347*, 126703. https://doi.org/10.1016/j.biortech.2022.126703

Zhao, M. L., Wang, J. X., Bian, X. K., Zhang, J., Han, Y. W., Xu, S. X., Lee, S. C., & Zhao, J. Z. (2023). Hexavalent chromium causes centrosome amplification by inhibiting the binding between TMOD2 and NPM2. *Toxicology Letters*, *380*, 12–22. https://doi.org/10.1016/j.toxlet.2023.03.008

Zheng, G., Kang, X., Ye, H., Fan, W., Sonne, C., Lam, S. S., Liew, R. K., Xia, C., Shi, Y., & Ge, S. (2024). Recent advances in functional utilisation of environmentally friendly and recyclable high-performance green biocomposites: A review. *Chinese Chemical Letters*, *35*(4), 108817. https://doi.org/10.1016/j.cclet.2023.108817